DEVELOPMENT OF AN ELECTROMYOGRAPHY SIGNAL OPERATED BIONIC-HAND WITH PRESSURE AND TEMPERATURE SENSING ABILITY

Shafa ISLAM*, **Samiha TASMIHA***, **Md Sayem Hossain BHUIYAN***, **Shadman Tajwar SHAHID***

*Faculty of Mechanical Engineering, Military Institute of Science and Technology, Mirpur Cantonment, Dhaka-1216, Bangladesh

shafaislam49@gmail.com, samihatasmiha99@gamil.com, sayem@me.mist.ac.bd, shadman@me.mist.ac.bd

received 04 August 2025, revised 18 November 2025, accepted 27 November 2025

Abstract: This study presents the development of a surface electromyography (sEMG)-operated bionic hand equipped with pressure and temperature sensing capabilities. The primary objective is to restore functional hand movement and sensory feedback in amputees through a low-cost, customizable prosthetic system. The proposed device utilizes surface EMG signals acquired using a MyoWare sensor to control finger and joint actuation, with an Arduino UNO as the central processing unit. Pressure and thermal sensors are integrated to detect grip force and object temperature during real-time interactions. The bionic hand was designed using SolidWorks and fabricated via 3D printing with PLA material. Experimental validation demonstrates 98.2% motion accuracy, sub-second response time, and full repeatability in multiple test cycles. Despite minor limitations such as a 2% nominal error and susceptibility to environmental factors, the system shows no overheating or maintenance issues. The device represents a significant advancement in combining intuitive control with sensory feedback, making prosthetics more functional, responsive, and accessible.

Keywords: sEMG, bionic hand, sensory feedback, pressure sensor, temperature sensor, MyoWare, 3D-printed prosthetic

1. INTRODUCTION

1.1. Background and Importance

The human hand is a highly complex and versatile organ, playing an essential role in interaction, manipulation, and communication. The loss of a hand due to trauma, congenital conditions, or surgical amputation can result in significant psychological and physical disability, severely impacting quality of life [1]. Traditional prosthetic devices often focus on cosmetic restoration or basic mechanical functions, offering limited support in restoring dexterity and sensory perception.

Bionic hands—robotic prostheses controlled through user input—have emerged as a transformative solution to restore hand functionality. These devices enable intuitive control over finger and joint movement, aiming to replicate natural hand biomechanics. With the advancement of bioengineering and human-machine interfaces, electromyography (sEMG)-based control systems have become a popular method for prosthetic actuation due to their non-invasive nature and high responsiveness [2, 3].

1.2. Medical Relevance and Role of sEMG Sensors

Surface sEMG sensors detect the bioelectrical activity of muscles when they contract, making them suitable for interpreting voluntary motion signals from the user's residual limb [4]. One such sensor, the MyoWare sEMG module, offers a compact and affordable platform for controlling bionic limbs through muscle activity [5]. When placed over residual muscles, these sensors can detect movement intentions, allowing real-time prosthetic response. Moreover, sEMG sensors contribute significantly to rehabilitation by supporting neuromuscular re-education and reducing muscular atrophy [6].

Incorporating sensory feedback such as pressure and temperature detection enhances user interaction with the environment, facilitating safer and more precise control over grip strength, object handling, and thermal hazards [7]. As highlighted in recent works, prostheses equipped with feedback systems not only enhance physical interaction but also improve user satisfaction and embodiment [8].

1.3. Existing Technologies and Limitations

Numerous actuation mechanisms have been explored to enhance the performance of bionic hands. Shape Memory Alloys (SMA) provide compactness and force efficiency but suffer from power inefficiency and thermal lag [9]. Twisted string actuators allow lightweight designs with efficient energy transmission but often lack precision [10]. Soft robotic hands offer greater flexibility and adaptability, though challenges persist in achieving natural motion and long-term durability [11]. Research into embedded actuators and integrated sensing has further pushed the field toward multifunctional designs [12].

Despite these innovations, high production costs, mechanical complexity, and limited sensory integration hinder the widespread adoption of these devices—particularly in resource-constrained environments [13]. Accessibility remains a significant barrier, with

many high-performance prosthetics priced beyond the reach of the average user. Furthermore, the reliability and repeatability of sEMG signal interpretation are affected by electrode placement,user fatigue, and environmental factors [14].

1.4. Recent Advances and Research Gap

A review study carried out by Zhu et al. [15] reported that upper-limb prosthetic control still faces major obstacles such as unintuitive control, missing sensory feedback, and limited sensor modalities. However, the advanced sEMG-based gesture recognition systems have achieved high accuracy using optimized classifiers [16 - 18], and hybrid systems using deep learning and machine learning algorithms with the help of various sensory modalities like thermal feedback [19] or image-EMG fusion [20]. Atashzar et al. [21] note that while sEMG-based control offers promising avenues, many systems lack robustness and generalizability across users. Additionally, Yamada et al. [22] demonstrated the integration of haptic feedback in sEMG-controlled hands, suggesting this approach can significantly improve real-time awareness and safety. From a user-centered design perspective, Peerdeman et al. [23] underscore the importance of intuitive interfaces and the psychological benefits of prostheses that feel more lifelike.

1.5. Research Objective and Novelty

In response to these challenges, this study proposes a low-cost, 3D-printed bionic hand controlled via sEMG signals and equipped with pressure and temperature sensing capabilities. The goal is to enhance interaction fidelity, ensure rapid response time, and maintain structural simplicity while improving sensory awareness. Unlike conventional systems that focus solely on motion replication, the integration of dual-mode sensory feedback aims to provide amputees with a more natural and intuitive prosthetic experience.

This research offers several contributions: a lightweight and customizable hand structure, high-accuracy motion control using MyoWare sEMG signals, real-time pressure and thermal sensing, and a system that balances functionality with affordability and repeatability. It marks a significant step toward the development of practical, biomimetic prosthetic devices.

2. BIONIC ARM DESIGN

A precise mechanical model that can meet human demands must be created in order to construct a prosthetic arm for amputees who have lost a limb. Since creating a prosthetic limb was the primary goal, some biological aspects of the human arm were taken into account right away. When designing the bionic arm, consideration was given to features including wrist mobility, grasping and holding, and independent finger manipulation. A 3D printer can be used to construct the entire design.

2.1. Anthropometric Measurement

The primary objective was to create a prosthetic arm that could perform all the functions of a real human hand, including feeling touch. Because prosthetic arms don't have the same neural networks as human hands, amputees can't sense what it's like to touch things. By simulating tactile sensations, vibrators can improve the user's sense of an object's weight and texture [13]. Perceiving hot or cold objects is a component of thermal sensation, another sensory feedback. By incorporating these technologies with prosthetics, users will be able to sense temperature changes on their skin, improving their sensory experience [24]. These capabilities were taken into account when developing the arm, and sensors like FSR and thermal sensors were housed in the palm. Since anthropometric measurements were acquired from a volunteer for the experiment, no ethical permits were needed. The longitudinal dimensions for each component taken into account during design are shown in Table 1.

Tab. 1. Anthropometric data

Anthropometric variables	Dimension[mm]
Index Finger Tip	37
Index Finger Middle	38
Index Finger Bottom	39.90
Pinky Finger Tip	27.92
Pinky Finger Middle	30.40
Pinky Finger Bottom	31.85
Thumb Tip	31.50
Thumb Middle	34
Thumb Lower	44.5 (Palm End)-24(Thumb lower end)
Palm	97.45
Wrist Forearm Section (2)	30.85
Upper Forearm	110
Middle Forearm Section	112

2.2. CAD Design of the Bionic Hand Structure

This project's primary goal was to create a bionic arm with human-like capabilities. Numerous open-source resources were taken into account when designing the arm. The following specifications had to be met by the design: for human fingers, each finger should comprise three segments, with channels allowing artificial tendons, such as fishing wire, to pass through and form a closed loop. These segments will be joined by shafts that resemble bicycle sprockets, and the palm needs to have openings for the prosthetic tendons. There should also be locations for the sensors to be installed, as well as housing specifically for the servos and battery. To keep the tendons from twisting, it's crucial to ensure distinct perforations.

A 3D model was designed by integrating features from several publicly available open-source prosthetic hand concepts, with extensive modifications to dimensions, tendon path, and actuator housing to suit the experimental objectives. Figure 1(a) shows

lower forearm, Figure 1(b) shows middle forearm, Figure 1(c) shows wrist, Figure 1(d) shows palm, Figure 1(e) shows thumb, Figure 1(f) shows finger. Figure 2 below shows the SOLIDWORKS CAD model.

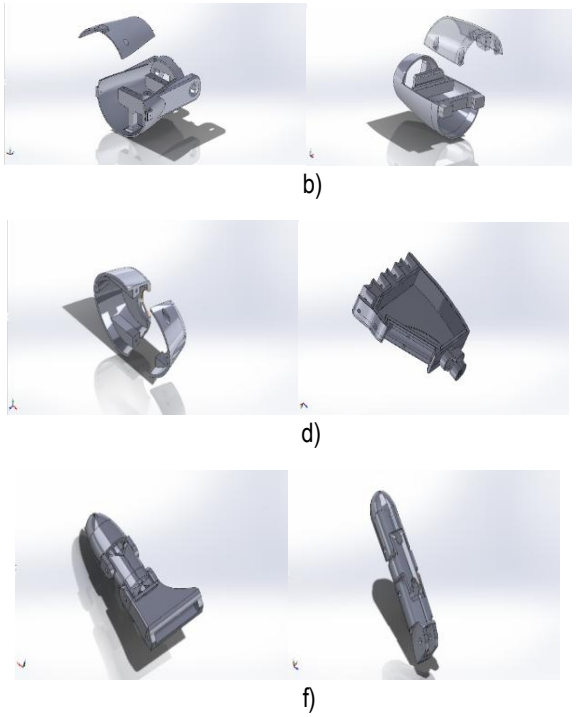

Fig.1. Parts of the bionic-hand: a) lower forearm, b) middle forearm, c) wrist, d) palm, e) thumb, and f) finger

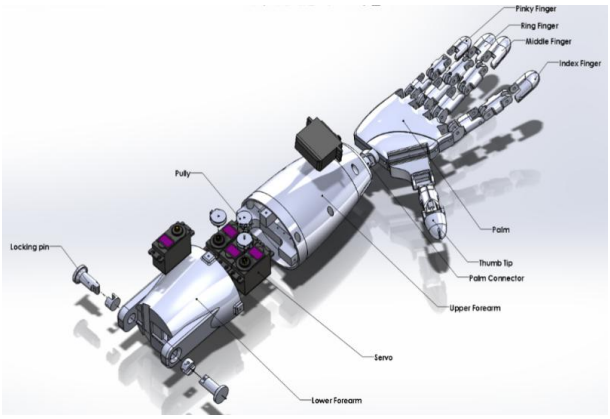

Fig. 2. Exploded view of the model

The various parts of the Bionic hand were 3D printed using PLA filament. Together with the electrical and electronic components, the 3D-printed prosthetic arm weighed 970g in total. Despite certain dimensional issues that were found after the components were 3D printed, this design complied with all the specifications. Friction between two moving pieces had a tendency to lock fingers. Thus, the measurements were altered. The hole size is extended to 3mm for sprockets, which were used to improve joint strength. The fingers had to remain parallel to the palm when there was no stress. To prevent rearward movement about the palm in these situations, the design had to be changed. Figure 3 below displays the closed loops created by the artificial tendons.

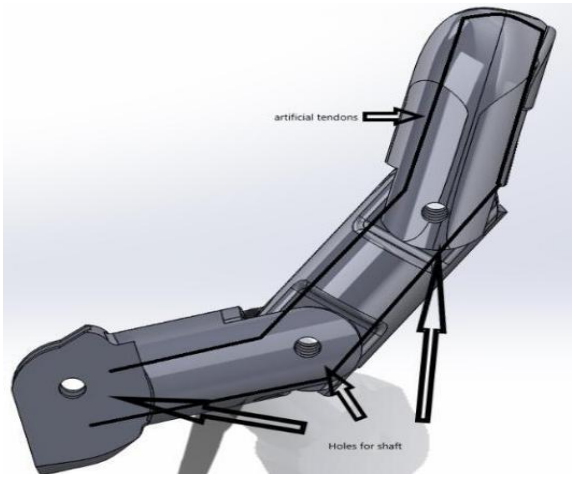

Fig. 3. String-operated index finger construction

3. CONTROL SYSTEM DESIGN FOR THE BIONIC HAND

The process of control system design has been comprised with circuit design and selection of electrical and electronic components for the prosthesis.

3.1. Electronic Components Selection

Table 2 below lists the electrical and electronic parts chosen for the prosthesis control system.

Tab. 2. Component list

Components	Specifications
Power Source	2200mah,11.1v rechargeable Lithium polymer battery
Microcontroller	Arduino UNO R3
sEMG Sensor	MYOWARE V2.0 (Sparkfun)
Vibration Motor	3V,10mm coin motor
Pressure Sensor	FSR402
Servo Voltage regulator	LM2596 DC-DC
Thermal Sensor	MLX90614
Temperature regulator	Heated pad
Servo Motors	MG996R(Towerpro)

Real-time control of prosthesis movements is made possible by the MyoWare V2, which uses sEMG sensors to identify electrical activity from muscle contractions [25]. Complex motion commands like elbow flexion and wrist rotation are made possible by its ability to record signals from several muscles, including the triceps and biceps [26]. The servos are then moved by the sensor's ability to identify the band at which the muscle is flexed and to produce more voltage for greater flex. The bionic arm's palm was equipped with a

DOI 10.2478/ama-2025-0082

Force Sensitive Resistor (FSR 402) to simulate touch. Robotic grippers frequently use FSRs to monitor contact forces, which allows for fine control while performing grasping tasks [27]. The amputee's hand is equipped with a coin-shaped motor that reads signals from FSR402. The amputee received vibrotactile feedback from this motor. The MLX90614 provides safe temperature readings by detecting infrared radiation produced from objects [28]. MG996R servos were employed to enhance grabbing capabilities. The main computer in this system is an Arduino Uno R3.

3.2. Circuit Design

The schematic diagram of the entire circuitry system was constructed using Cirkit Designer. A thermal sensor (MLX90614) and an additional Arduino UNO microcontroller were utilized to allow the prosthesis to sense temperature. The wiring of the entire system is depicted in Figure 4(a) shows circuit diagram for servo control and Figure 4(b) shows circuit diagram for thermal sensor and heating pad.

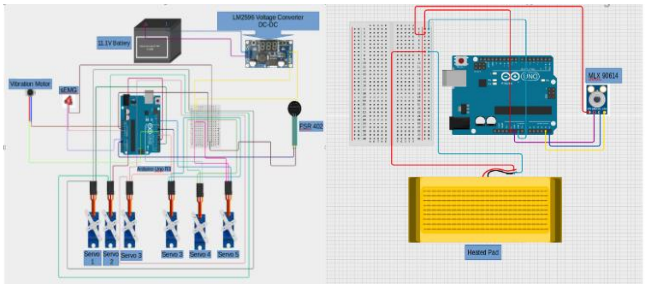

a) b)

Fig. 4. Circuitry system: a) Circuit diagram for movement control, b) Circuit design of thermal sensor and heating pad control

4. CONTROL SYSTEM

4.1. Mathematical Model

Before the control system was created, a mathematical model of the index finger's kinetics—the movement that needs to be controlled—was created. The force on the tip of the index finger was measured while it was fully extended. Figure 5(a) shows tension generated on the string by the servo, Figure 5(b) and 5(c) shows the force diagram of the identical four fingers and the thumb. The yellow lines are the path that the tendons follow through the holes of each finger. The mathematical model below calculates the forces generated in each finger.

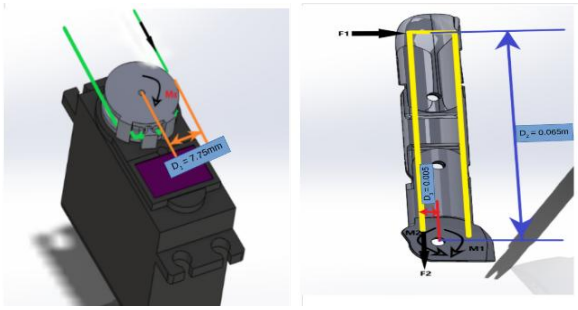

a) b)

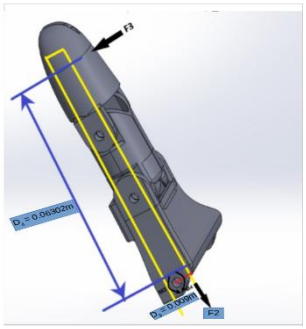

c)

Fig. 5. Force diagram: a) tension generated on the string by the servos, b) index finger, c) force diagram of thumb

Moment = Force × Perpendicular Distance

M=Fd

The tendon creates a moment around each finger joint in this mechanism. Because of its greater distance from the applied force, the knuckle joint experiences the highest moment. Consequently, the maximum liftable weight at the fingertip is governed by the rotating force at the knuckle. Moments M1 and M2 will balance when the maximum load is applied.

To begin the computation, the tendon's tensile force must be determined. The MG996R servo has a stall torque of 10 kg-cm (≈ 1 N·m). A custom 3D-printed tendon holder was attached to the servo's rotating shaft of diameter D1 = 0.00775 m. The bionic hand includes four identical fingers, each designed to exert equal force when actuated. As shown in Fig. 5 (b), the torque generated by the servo is transmitted through the tendon to the finger knuckle, producing a moment about the joint and a corresponding linear force F2 . The diameter of the finger knuckle is D3 = 0.005m.The distance from the finger joint (knuckle) to the fingertip is D2 = 0.065 m.

Assuming static equilibrium and negligible energy losses in the tendon system, the relationship between applied torque τ, fingertip force F1 and their respective moment arms is:

$$F_1 * D_1 = F_2 * D_2$$

Substituting the values below

$$F_2 = \frac{\tau}{D_1} \quad [29]$$

$$F_2 = \frac{1NM}{0.00775m} = 129N$$

$$F_1 * D_1 = F_2 * D_3$$

$$F_1 = \frac{129N*0.005m}{0.065m} = 9.92N$$

$$m_1 = \frac{9.92}{9.81} \simeq 1.01kg$$

Hence, when the fingers are fully extended, approximately 129 N of tension can be transmitted to each fingertip, enabling a lift of about 1.01 kg per finger. As the fingers curl, the perpendicular distance to the knuckle decreases (by roughly 30 mm), thereby increasing the effective lifting capability. Under this configuration, each finger can lift about 2.2 kg, and the combined lifting capacity of four fingers becomes 8.78 kg.

For the thumb (Fig. 5c), the string tension acts along a line similar to that of the other fingers but with slightly different geometry. Using D4 = 0.0632 m and D5 = 0.009 m, the calculation gives:

$$F_3 * D_4 = F_2 * D_5$$

$$F_3 = \frac{129N * 0.009m}{0.0632m} = 18.4N$$

$$m_2 = \frac{18.4}{9.81} \simeq 1.87kg$$

Adding the thumb contribution to the four fingers yields a theoretical total lifting capacity of approximately 10.6 kg.

It should be noted that this value represents an idealized theoretical maximum under loss-free assumptions. From experiment, it has been observed that the friction at joints, tendon elongation, and servo torque derating under continuous load reduce the effective lifting capacity to about 7 kg. These discrepancies are typical for tendon-driven systems and will be addressed in future work through improved tendon routing, reduced friction, and use of higher-torque servos.

Symbols	Descriptions	Value
τ	Servo stall torque (MG996R)	1.0 N·m
D_1	Shaft radius used for tendon tension	0.00775 m
D_2	Knuckle-to-fingertip distance	0.065 m
D_3	Knuckle Diameter	0.005 m
D_4	Knuckle Diameter(thumb)	0.009 m
F_2	Tendon tension	129 N
F_1	Fingertip force (four fingers)	9.92 N
F_3	Fingertip force(thumb)	18.4N
m_1	Mass per finger	1.01 kg
m_2	Thumb mass-equivalent	1.87 kg
Total (curled)	4×m1,curled + m2	10.6 kg

The bionic arm can theoretically lift 10.6 kg when all the forces are combined. This could change, though, because of things like friction, loosened tendons, or friction in the joints from long materials (which were manually removed with sandpaper). But in real-world experiments, the arm could barely raise 7 kg with four fingers. Weights were added from a small scale to a larger scale. All the experiments were conducted for two patterns, where

pattern 1 = relaxed state (no flexion)

pattern 2 = active grip (flexion)

a) b) c)

Fig. 6. Functional demonstration of lifting ability: a) Hand in no grip position(no lifting force), b) lifting the weight horizontally, c) lifting the weight vertically

Figure 6 (a) shows the hand in pattern 1, Figure 6(b) shows the lifting in horizontal position for pattern 2 and Figure 6(c) shows lifting the weight vertically for pattern 2. Note that the thumb did not contributed to lifting.

Over time, it is found that as the joints loosen up, the overall assembly acquires far more agility. Over time, the shafts also rotate more easily, and the tension is transferred through the tendons with more accuracy.

5. CONTROL ALGORITHM

The proposed system is actuated through muscular flexion, with the MYOWARE muscle sensor capturing the electromyographic (sEMG) signal from the user's muscle activity. This signal is converted from an analog to a digital format and subsequently processed by a microcontroller (Arduino). The Arduino is programmed to monitor the sEMG signal in real time and initiate predefined control commands when the signal exceeds a specified threshold. Upon reaching this threshold, servo motors are activated to manipulate tension cables, enabling the bionic hand to execute a grasping motion. If the sEMG signal remains below the threshold, the initiation sequence is reset and awaits sufficient input. Once the hand comes into contact with an object, integrated pressure sensors detect the applied force and relay this information to a vibrotactile motor, which provides haptic feedback to the user. Additionally, a thermal sensor embedded in the system activates a heat pad when it detects proximity to a high-temperature object, enhancing environmental interaction awareness. Below is a rudimentary diagram of the signal flow between several components.

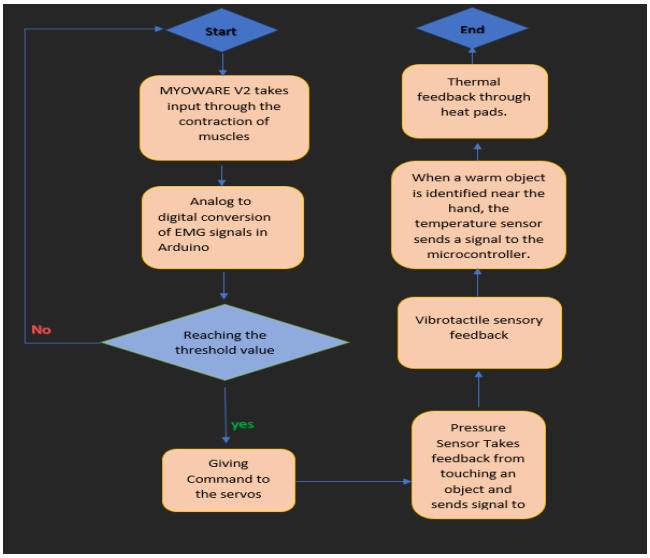

Fig. 7. Program Flow

6. PERFORMANCE TEST RESULTS

6.1. sEMG Data Acquisition and Analysis

Due to unavailability of volunteer amputees, data has been collected from a healthy subject. Data was extracted appropriately from the serial monitor of the Arduino IDE for the specific person in order to have control over fingers.

DOI 10.2478/ama-2025-0082

All the fingers had to cooperate in order to grip an object. In order to open and close all of the fingers simultaneously, sEMG signals were selected from the same person for the same setup.The sEMG data from the Myoware V2 is displayed in Fig. 8 below.

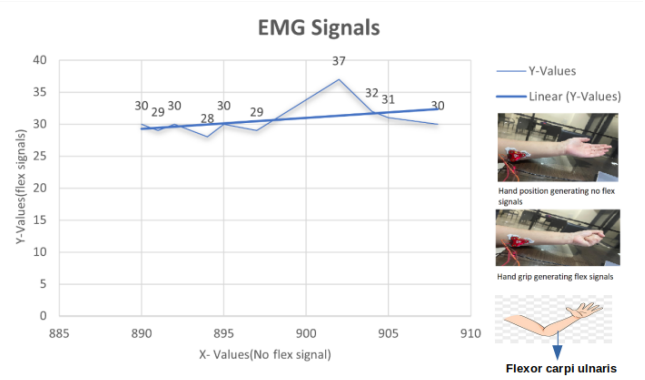

Fig. 8. sEMG Signals picked from Flexor carpi ulnaris for pattern 1 and pattern 2

The pattern 1 and pattern 2 signals linked to arm movements are represented by the X and Y values in Figure 8. Each movement causes these signals' lowest and maximum magnitudes to change. The sensor normally reports values in the range of 900 to 930 under optimal circumstances. However, as the trend line in Figure 8 illustrates, the sEMG data fluctuated at an RMS value of 30 when the muscle group to which it is linked was strongly flexed. The servo motors were operated based on the RMSE value of the recorded sEMG. Notably, it takes around 100 milliseconds for the signals to stabilize from optimal settings. A USB isolator was used to reduce noise while data extraction was taking place.

6.2. Controllability Test Data

For improved gripping ability, the servos have to react differently depending on the flex intensity. For example, in order to cling to an object, a higher gripping force may be needed at times. When the muscle is flexed more forcefully, the MYOWARE V2 can detect the signals. The values between idle flex intensity and high flex intensity are displayed in Fig. 9.

As illustrated in Figure 9, the recorded sEMG signal values during muscle flexion ranged between approximately 105 and 250. Given that the MG996R servo motor employed in this study is position-controlled rather than torque-controlled, a proportional mapping strategy was implemented wherein the servo's angular position was modulated based on the magnitude of the sEMG signal. Figure 9(b) shows at lower sEMG intensities, the servo was commanded to rotate to a smaller angle, resulting in a relatively loose grip. As the sEMG signal increased, the target angle was incrementally adjusted to simulate a stronger grasp. This behavior exploits the internal control mechanism of the servo, which inherently applies greater holding force when attempting to maintain a larger angle against external resistance. The control logic was configured such that the prosthetic fingers remained stationary for sEMG values below a threshold of 100. Once this threshold was exceeded, the servo initiated the grasping motion, and as the signal magnitude continued to rise, the servo advanced to progressively larger angular positions, thereby increasing the effective gripping force applied by the prosthetic hand. The values may differ from person to person, though, as these data were only collected from one specific subject. Physically, the arm could grasp small to medium sized objects of dimension between 80 mm to 300 mm with smooth and rough surfaces by pattern 2. Figure 10(a) shows holding an object with a rough surface, Figure 10(b) shows holding a smooth surface object. These two grips required all five fingers, whereas Figure 10(c) requires three fingers to hold the object.

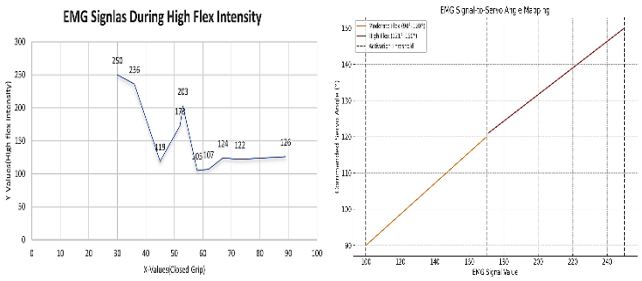

Fig. 9. Control of the servos: a) Signals picked while flexing the muscle with high intensity, b) sEMG signal to servo angle mapping

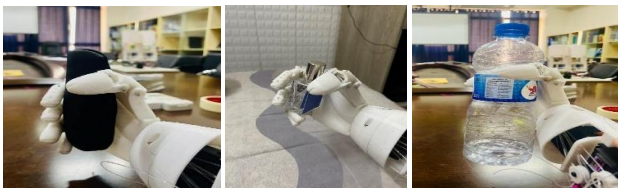

a) b) c)

Fig.10. Different object gripping capabilities:a) Holding an object with a rough surface (pattern 2), b) Holding an object with a smooth surface (pattern 2), c) gripping with three fingers (pattern 2)

As illustrated in Fig.10, the objects were held while the arm was resting on a table. 100% repeatability was discovered.

6.3. Pressure Sensing Ability Test Data

The goal was to give amputees sensory feedback each time they touched an object. Data was first gathered by touching the sensor's touchpad. You must first ascertain the supply voltage (e GG) and the analog voltage (e l) in order to compute the Force Sensing Resistor (FSR) resistance value in Newtons. The FSR sensor has a 5V supply voltage, and when it makes contact with the sensor surface, the analog voltage is determined by the sensor's output [5, 30]. Instructions on when to send a signal to the vibrator motor were required by the program. Various FSR readings were used to define various reactions. The Serial Monitor in the Arduino IDE software provided the data below, which is displayed in Table 3.

Tab. 3. Feedback from FSR

Sensor Input	Nature of Responses
500	Too sensitive (vibrator auto vibrates after each delay time)
700	Less sensitive (if something moves near the FSR touch pad vibrator vibrates)

900	For instance, environmental factors, ex, if the wind blows, FSR reads the signal and the vibrator vibrates
1000	The vibrator stopped vibrating due to movements, but was too responsive to touch.
1022	The response was good as only forcing the finger on the FSR would make the motor vibrate.
1100	The FSR touchpad needed to be pressed harder for a response in the vibrator

Following an iteration of the FSR readings, 1022 was determined to be the most appropriate value. The program designated this value as the threshold, and the vibrator motor would receive a write signal with a 500 ms delay anytime the FSR reading exceeded it. By evaluating the consequences of variances in surface electromyogram signals for various postures and motions, a data integration system may be put into place to increase system reliability [31].

6.4. Temperature Sensing Ability Test Data

Both ambient temperature and object temperature can be measured using the MLX90614 device. Different objects were positioned one centimeter from the sensor in order to determine their threshold temperature. To identify a hot object, a soldering iron was placed within the sensor's field of view. The data gathered during this procedure is shown in Figure 11(a). A sudden gradual rise in temperature can be seen in the graph near the soldering iron. Figure 11(b) shows the position of the temperature and pressure sensor. One is placed at the tip of the finger where small holes are created so that MLX90614 can capture heat signals, and FSR is placed on the palm so that the pressure generated during the grip can be calculated and accordingly the sensory feedback can be generated via vibrotactile motor.

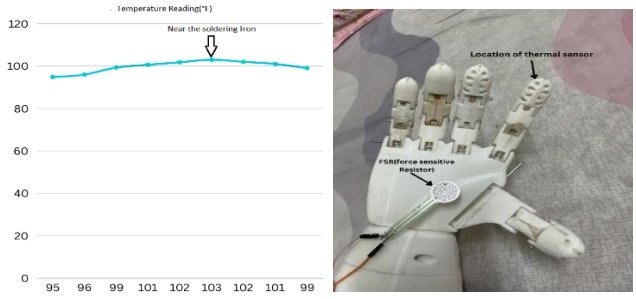

a) b)

Fig.11. Sensor location and data: a) thermal sensitivity data, b) location of the sensors

The temperature rose from 94°F to 101°F based on the value displayed in Fig. 11. In order to convey the signal to the heating pad, a threshold value of 100°F was established. As heat is gained or lost over time, the object's temperature changes. The physical relationship between temperature and other physical qualities can be effectively represented by optimizing model parameters and compensating for these oscillations in order to address mistakes in thermal sensor readings [29]. For a certain amount of time, the sensor could consistently detect items like ice cream and warm water. Following that, thresholds were established using the temperature readings from these items to send signals to the heating pad for heating. Unfortunately, it was not possible to create the feeling of coolness because of the restriction of utilizing just heating pads.

7. DISCUSSION

The printed pieces' precision and smoothness of movement are impacted by a friction problem that needs to be manually sanded. PLA is not appropriate for uses that are subjected to high temperatures or strong forces. The system takes 100 milliseconds to react to the MYOWARE signal, which may cause issues for quick responses. Because of its small memory, the Arduino Uno may have trouble with adaptive feedback systems. Although the thermal sensor provides heat input and the vibrator gives amputees the sensation of gripping objects, neither device provides tactile or variable pressure feedback. Furthermore, over time, the tendons of fishing wire may stretch, affecting durability and accuracy. The usefulness of the thermal sensor is limited because of its placement on the fingertip, which allows it to only sense heat from direct touch. The bionic hand picks up signals from the MYOWARE with 98% accuracy. The frequency with which the MYOWARE selected the RMS value 30, which was established as the threshold, is shown in Fig. 12.

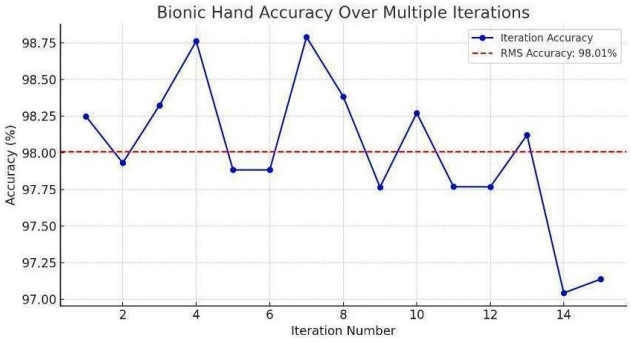

Fig.12. Accuracy of the system in responding to desired input signals

Fifteen consecutive grasp trials were conducted, where each trial comprised both pattern 1 and pattern 2 to see the overall performance of the system under multiple repetitions. In addition to this, the thermal sensor (MLX90614) and the force-sensitive resistor (FSR402) were also evaluated over the fifteen repetitions. During these tests, a soldering iron was positioned near the bionic hand to generate a controlled thermal stimulus, while a separate object was applied to the palm region containing the pressure sensor to assess tactile responsiveness. An approximately 98% overall accuracy was found in these sensor signals while doing the picking-up test simultaneously.

The primary objective of this study was to develop a bionic hand capable of sensing pressure and temperature. However, due to the limited number of available electrodes and the unwillingness of amputees to voluntarily participate in the experiment, testing the adaptability of the developed prototype has been hindered, allowed to perform only one grip pattern test.

8. CONCLUSIONS

This study successfully demonstrates the development of a low-cost, 3D-printed bionic hand controlled by electromyographic

(sEMG) signals, and enhanced with dual-mode sensory feedback through integrated pressure and temperature sensors. The system achieved its core objectives: accurate sEMG-based motion control using the MYOWARE sensor, real-time feedback responsiveness (1-second actuation with stability in under 100 ms), and a structurally simple yet functional prosthesis design. The combination of lightweight materials, modular components, and embedded sensory mechanisms enabled a natural and intuitive user interaction, moving beyond basic motion replication toward a more biomimetic experience.

Despite these achievements, the system presents certain limitations. The use of PLA in structural components introduces mechanical fragility under moderate loads, limiting long-term durability. Additionally, environmental sensitivity—particularly to water—and a nominal 2% error from sensor noise highlight the need for further refinement. These limitations, while not critical for initial functionality, must be addressed to improve robustness and expand the device's usability in daily-life scenarios.

Future work will focus on enhancing the mechanical resilience of the prosthetic hand by investigating alternative structural materials, such as reinforced polymers or flexible composites, and optimizing joint mechanisms for improved durability. Environmental robustness will also be addressed through the implementation of protective sealing techniques to ensure reliable operation under real-world conditions. On the sensory front, advanced signal processing methods will be explored to minimize noise and enhance the resolution of feedback signals. Furthermore, as the current study was conducted using a single amputee subject, future iterations will aim to generalize the system through the integration of machine learning algorithms capable of adapting to individual muscle activation patterns. This will enable broader applicability and personalization across diverse user profiles. Collectively, these advancements will build upon the current system's foundation, driving progress toward more universally adaptable, cost-effective, and biomimetic prosthetic technologies.

REFERENCES

1. Said S, Boulkaibet I, Sheikh M, Karar AS, Alkork S, Nait-Ali A. Machine-learning-based muscle control of a 3D-printed bionic arm. Sensors (Basel) [Internet]. 2020;20(11):3144. Available from: http://dx.doi.org/10.3390/s20113144
2. Whenish R, Antony MM, Balaji T, Selvam A, Ramprasath LS, Velu R. Design and performance of additively manufactured lightweight bionic hand. In: Proceedings Of The 14th Asia-Pacific Physics Conference. AIP Publishing; 2021.
3. Li Z, Li H, Wang D, Wang L, Zeng X, Li Y. The development of a two-finger dexterous bionic hand with three grasping patterns-NWAFU hand. J Bionic Eng. 2020;17(4):718–31.
4. Mangukiya Y, Purohit B, George K. Electromyography (EMG) sensor controlled assistive orthotic robotic arm for forearm movement. In2017 IEEE Sensors Applications Symposium (SAS). IEEE. 2017; 1-4.
5. Babu D, Mahadevappa M, Venkatesh P, Venkatesan V, Mohamed AS. 3D printed prosthetic robot arm with grasping detection system for children. Int J Adv Sci Eng Inf Technol. 2023;13(1):226–34.
6. Iqbal NV, Subramaniam K, P. SA. A review on upper-limb myoelectric prosthetic control. IETE J Res [Internet]. 2018;64(6):740–52. Available from: http://dx.doi.org/10.1080/03772063.2017.1381047
7. Tavakoli M, Batista R, Netto A, Neves J. The UC Softhand: lightweight adaptive bionic hand with a compact twisted string actuation system. Actuators. 2015;5(1).
8. Cipriani C, Segil JL, Birdwell JA, ff Weir RF. Dexterous control of a prosthetic hand using fine-wire intramuscular electrodes in targeted extrinsic muscles. IEEE Trans Neural Syst Rehabil Eng [Internet]. 2014;22(4):828–36. Available from: http://dx.doi.org/10.1109/TNSRE.2014.2301234
9. Simone F, York A, Seelecke S. Design and fabrication of a three-finger prosthetic hand using SMA muscle wires. In: Lakhtakia A, Knez M, Martín-Palma RJ, editors. Bioinspiration, Biomimetics and Bioreplication. SPIE; 2015.
10. Krausz NE, Rorrer RAL, Weir RF ff. Design and fabrication of a six degree-of-freedom open source hand. IEEE Trans Neural Syst Rehabil Eng [Internet]. 2016;24(5):562–72. Available from: http://dx.doi.org/10.1109/tnsre.2015.2440177
11. Alves S, Babcinschi M, Silva A, Neto D, Fonseca D, Neto P. Integrated design fabrication and control of a bioinspired multimaterial soft robotic hand. Cyborg Bionic Syst [Internet]. 2023;4:0051. Available from: http://dx.doi.org/10.34133/cbsystems.0051
12. She Y, Li C, Cleary J, Su HJ. Design and fabrication of a soft robotic hand with embedded actuators and sensors. Journal of Mechanisms and Robotics. 2015;7(2):021007.
13. Fras J, Althoefer K. Soft biomimetic prosthetic hand: Design, manufacturing and preliminary examination. In: 2018 IEEE/RSJ International Conference on Intelligent Robots and Systems (IROS). IEEE; 2018.
14. Clement RGE, Bugler KE, Oliver CW. Bionic prosthetic hands: A review of present technology and future aspirations. Surgeon [Internet]. 2011;9(6):336–40. Available from: http://dx.doi.org/10.1016/j.surge.2011.06.001
15. Jiang N, Chen C, He J, Meng J, Pan L, Su S, Zhu X. Bio-robotics research for non-invasive myoelectric neural interfaces for upper-limb prosthetic control: a 10-year perspective review. National science review. 2023;10(5):nwad048.
16. Zhang M, Liu S, Li X, Qu L, Zhuang B, Han G. Improving sEMG-based hand gesture recognition through optimizing parameters and sliding voting classifiers. Electronics. 2024;13(7):1322.
17. Hellara H, Barioul R, Sahnoun S, Fakhfakh A, Kanoun O. Comparative study of semg feature evaluation methods based on the hand gesture classification performance. Sensors. 2024;24(11):3638.
18. Kang S, Kim H, Park C, Sim Y, Lee S, Jung Y. sEMG-based hand gesture recognition using binarized neural network. Sensors. 2023;23(3):1436.
19. Xie A, Li C, Chou CH, Li T, Dai C, Lan N. A hybrid sensory feedback system for thermal nociceptive warning and protection in prosthetic hand. Frontiers in Neuroscience. 2024;18:1351348.
20. Mersinkaya I, Kavsaoglu AR. A Data Acquisiton System with sEMG Signal and Camera Images for Finger Classification with Machine Learning Algorithms. Engineering, Technology&Applied Science Research. 2024;14(2):13554-8.
21. Atashzar SF, Patel RV, Arami A, Pedram A. Prosthetic hand control using sEMG: a review on existing methods, challenges, and future directions. Biomed Signal Process Control. 2021;63.
22. Yamada H, Shibata T, Seki M, Watanabe K. Development of an sEMG-controlled prosthetic arm with haptic feedback. Robot Auton Syst. 2019;121.
23. Peerdeman B, Boere D, Witteveen H, Hermens H, Stramigioli S, Rietman H, Veltink P, Misra S. Myoelectric forearm prostheses: State of the art from a user-centered perspective. Journal of rehabilitation research and development. 2011;48(6):719-38.
24. Park W, Yu X. Simplified Closed-Loop Thermal Feedback System in Flexible form Factor for Prosthesis. In2023 IEEE 23rd International Conference on Nanotechnology (NANO) 2023; 311-316.
25. Kadhim AA, Sattar MA, Waleed AS. Prosthetic hand control using wearable gesture armband based on surface electromyography.
26. Sattar NY, Syed UA, Muhammad S, Kausar Z. Real-time EMG signal processing with implementation of PID control for upper-limb prosthesis. In 2019 IEEE/ASME International Conference on Advanced Intelligent Mechatronics (AIM) 2019;120-125.
27. Sadun AS, Jalani J, Sukor JA. Force Sensing Resistor (FSR): a brief overview and the low-cost sensor for active compliance control.

InFirst international workshop on pattern recognition. SPIE. 2016; 10011:222-226.
28. Arifuzzaman M, Shipon MR, Akhi JA, Sejuti SY, Rahman MT, Khan MA. Design and implementation of thermal sensor based temperature measuring robot using Arduino Uno.
29. Lu S, Tessier R, Burleson W. Collaborative calibration of on-chip thermal sensors using performance counters. InProceedings of the International Conference on Computer-Aided Design 2012; 15-22.
30. Kim JJ, Kim J, Lee J, Shin J. Influence of lifestyle pattern on preference for prosthetic hands: understanding the development pathway for 3D-printed prostheses. J Clean Prod. 2022;379:134599.
31. Veer K. Interpretation of surface electromyograms to characterize arm movement. Instrumentation Science&Technology.2014; 42(5): 513-21.

Shafa Islam: https://orcid.org/0009-0000-8080-4495
Samiha Tasmiha: https://orcid.org/0009-0005-9702-2680
Md Sayem Hossain Bhuiyan: https://orcid.org/0000-0002-4233-3730
Shadman Tajwar Shahid: https://orcid.org/0009-0006-9174-3388